SCIENCE CHINA
Technological Sciences

February 2012 Vol.55 No.2: 445–450
doi: 10.1007/s11431-011-4681-9

Large magnetocaloric effect in metamagnetic HoPdAl

XU ZhiYi & SHEN BaoGen*

State Key Laboratory for Magnetism, Institute of Physics, Chinese Academy of Sciences, Beijing 100190, China

Received August 31, 2011; accepted October 18, 2011; published online December 28, 2011

Magnetic properties and magnetocaloric effects (MCEs) of the HoPdAl compounds with the hexagonal ZrNiAl-type and the orthorhombic TiNiSi-type structures are investigated. Both the compounds are found to be antiferromagnet with the Néel temperature T_N=12 and 10 K, respectively. A field-induced metamagnetic transition from antiferromagnetic (AFM) state to ferromagnetic (FM) state is observed below T_N. For the hexagonal HoPdAl, a small magnetic field can induce an FM-like state due to a weak AFM coupling, which leads to a high saturation magnetization and gives rise to a large MCE around T_N. The maximal value of magnetic entropy change (ΔS_M) is −20.6 J/kg K with a refrigerant capacity (RC) value of 386 J/kg for a field change of 0–5 T. For the orthorhombic HoPdAl, the critical field required for metamagnetic transition is estimated to be about 1.5 T, showing a strong AFM coupling. However, the maximal ΔS_M value is still −13.7 J/kg K around T_N for a field change of 0–5 T. The large reversible ΔS_M and considerable RC suggest that HoPdAl may be an appropriate candidate for magnetic refrigerant in a low temperature range.

HoPdAl compound, magnetocaloric effect, metamagnetic transition

Citation: Xu Z Y, Shen B G. Large magnetocaloric effect in metamagnetic HoPdAl. Sci China Tech Sci, 2012, 55: 445–450, doi: 10.1007/s11431-011-4681-9

1 Introduction

Magnetic refrigeration based on the magnetocaloric effect (MCE) is expected to be a promising alternative technology to the conventional gas compression refrigeration due to its higher energy efficiency and friendly environment. In order to obtain the magnetic refrigerant materials with a large magnetic entropy change (ΔS_M), the MCEs in magnetic materials have been investigated extensively [1–4]. Giant ΔS_M around the transition temperatures has been observed in many materials, each of which experiences a first-order phase transition [1–9]. From the viewpoint of practical applications, the rare earth (*R*)-based intermetallic compounds exhibiting large MCEs at lower temperatures are potential magnetic refrigerants for the gas liquefiers. Recently, much attention has also been paid to the *R*-based compounds with low-temperature phase transitions. Some intermetallic compounds, such as *R*CoAl [10], HoNiAl [11], DyCuAl [12], HoCuSi [13], Er_3Co [14], $DyNi_2$ [15], ErGa [16], etc., have been found to exhibit giant MCEs around their transition temperatures.

The ternary rare-earth compounds with the *R*PdAl composition have been investigated extensively in the past few decades due to their interesting physical properties. It was found that the crystal structure of *R*PdAl was sensitive to the history of its treatment process. The rapidly cooled and high-temperature (~1050°C) annealed samples crystallize in a hexagonal ZrNiAl-type structure (metastable high-temperature modification (HTM)), while the low-temperature (~750°C) annealed sample has an orthorhombic TiNiSi-type structure (stable low-temperature modification (LTM)) [17]. An isostructural phase transition from a high temperature modification HTM I phase to a low temperature modification HTM II phase in the metastable HTM of GdPdAl and TbPdAl was found [18, 19] for the samples crystallizing in

*Corresponding author (email: shenbg@aphy.iphy.ac.cn)

the hexagonal structure. However, the measurements of the lattice parameters, the electrical resistivity and the magnetic properties for DyPdAl and HoPdAl show no isostructural transition [20, 21]. For GdPdAl and TbPdAl, the strong molecular field produced by Gd and Tb both act on the Pd atoms and may polarize them. It is accompanied by an insignificant depletion of the occupied narrow Pd 4d band [22]. The density of states at the Fermi level increases and the magnetic moment is enhanced. However, an increase of magnetic moment is observed neither for DyPdAl nor for HoPdAl, indicating that Pd is non-magnetic and does not contribute to the density of states at the Fermi level [21]. The *R*PdAl compounds exhibit complex magnetic structures and possess different magnetic-phase transitions at low temperatures [18–25], which induce interesting magnetocaloric properties [26, 27]. In this paper, we report on the magnetic properties and the MCEs of HoPdAl compound. Large ΔS_M and considerable refrigerant capacity (RC) around the Néel temperature (T_N) are observed in HoPdAl.

2 Experimental

Polycrystalline HoPdAl was prepared by arc melting in a high-purity argon atmosphere. The purities of starting materials were better than 99.9%. The ingot was turned over and remelted several times to ensure its homogeneity. The metastable HTM was prepared by annealing as-cast material at 1080°C for 12 days and rapidly quenching to room temperature. The stable LTM was prepared by annealing as-cast material at 750°C for 50 days. X-ray diffraction (XRD) measurement on powder sample was performed by using Cu Kα radiation to identify the crystal structure. Magnetization was measured as a function of temperature and magnetic field by using a superconducting quantum interference device (SQUID) magnetometer. The temperature dependent magnetizations were measured in both zero field-cooled (ZFC) and field-cooled (FC) processes in order to determine the magnetic reversibility and the magnetic transition temperature. With the sample cooled down to 2 K in a zero field, the heating curve from 2 to 300 K was measured in a magnetic field of 0.01 T and the cooling curve from 300 to 2 K was measured also in the same field. The Néel temperature of the sample was defined as the temperature at which the maximum of *M*-*T* curve occurs. In order to determine the ΔS_M, the isothermal magnetization curves were measured by the SQUID magnetometer with magnetic fields up to 7 T at different temperatures.

3 Results and discussion

The powder XRD patterns of HoPdAl compounds were measured at room temperature. The Rietveld fitted results show that both the sample annealed at 1080°C for 12 days and the as-cast sample have a hexagonal ZrNiAl-type structure with space group $P\bar{6}2m$ (metastable HTM), while the samples annealed at 750°C for 50 days exhibit an orthorhombic TiNiSi-type structure with space group *Pnma* (stable LTM). Figures 1(a) and (b) show the Rietveld fitted XRD patterns of the hexagonal and the orthorhombic HoPdAl, respectively. As can be inferred from the difference in plot between the observed and the calculated patterns, both the samples are of single phase, and no impurity phase is observed. From the refinement result, the lattice parameters are determined to be a=7.1857(5) Å and c=3.9320(9) Å with the remaining factors being R_p=7.56%, R_{wp}=10.51%, and R_{exp}=1.59% for the hexagonal sample, and a=6.8527(4) Å, b=4.4037(9) Å and c=7.7242(8) Å with R_p=10.77%, R_{wp}=13.97%, and R_{exp}=5.84% for the orthorhombic sample, which are almost the same as those in ref. [17].

Figures 2(a) and (b) show the temperature dependences of zero-field-cooling (ZFC) and field-cooling (FC) magnetizations for the hexagonal and the orthorhombic HoPdAl under a magnetic field of 0.01 T. The results in Figure 2(a)

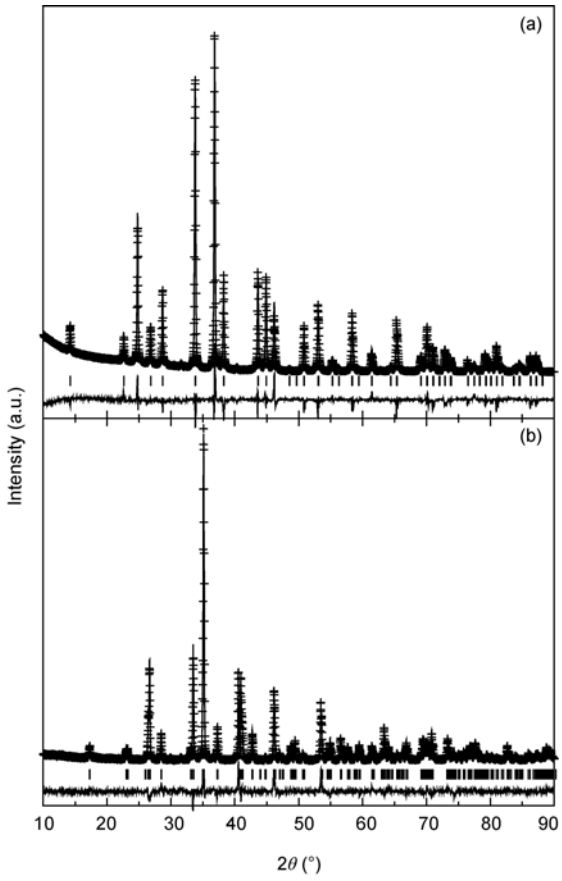

Figure 1 Rietveld refined powder X-ray diffraction patterns of (a) the hexagonal HoPdAl and (b) the orthorhombic HoPdAl at room temperature. The observed data are indicated by crosses and the calculated profile is the continuous line overlaying them. The short vertical lines indicate the angular positions of the Bragg peaks of the hexagonal and the orthorhombic HoPdAl, respectively. The lower curve shows the differences between the observed intensities and the calculated intensities.

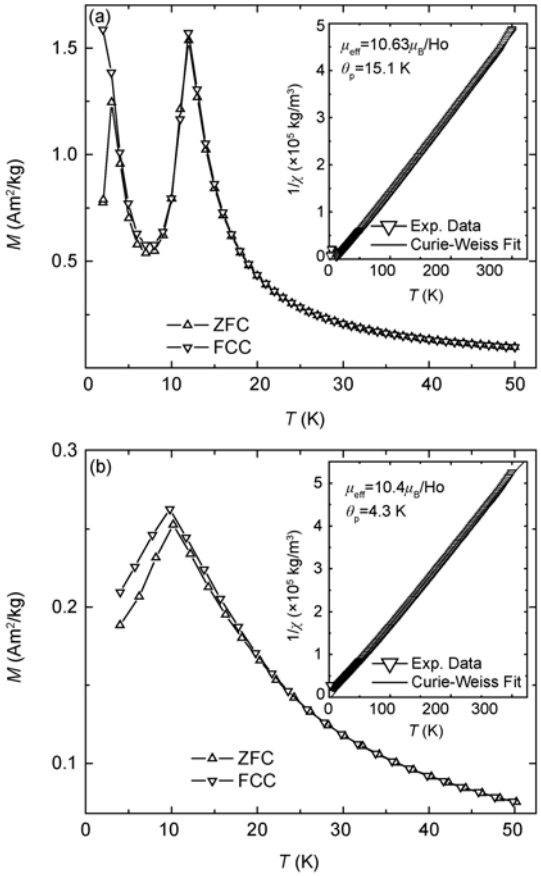

Figure 2 Temperature dependences of magnetization for (a) the hexagonal HoPdAl and (b) the orthorhombic HoPdAl in both zero field-cooled and field-cooled processes under a magnetic field of 0.01 T. The inset shows the reciprocal magnetic susceptibility (χ^{-1}) as a function of temperature at 0.01 T magnetic field.

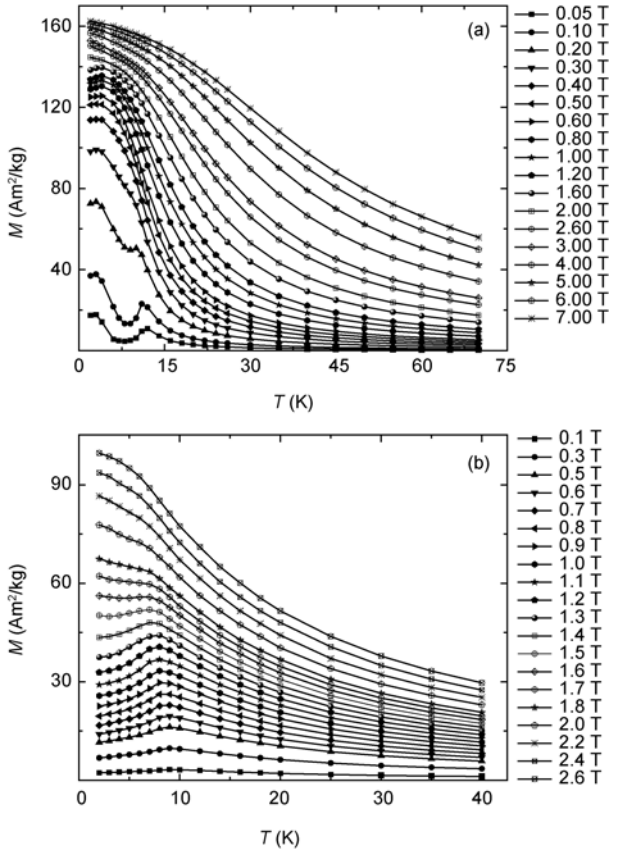

Figure 3 Temperature dependences of magnetization for (a) the hexagonal HoPdAl and (b) the orthorhombic HoPdAl in different magnetic fields.

show that the hexagonal HoPdAl undergoes two successive magnetic phase transitions at T_N=12 K and T_t=4 K, respectively. The change in magnetization around T_N is believed to be an indication of a second-order antiferromagnetic (AFM)-paramagnetic (PM) phase transition as temperature increases. The phase transition at T_t, which is not observed in the thermomagnetic measurements of previous work [21], is associated with the AFM structure transition as the case observed in TbPdAl [26]. It is clearly observed from Figure 2(b) that the orthorhombic HoPdAl has only an AFM-PM phase transition at T_N=10 K. There is a small difference in T_N between the hexagonal HoPdAl and the orthorhombic HoPdAl, which is different from those observed in TbPdAl, where both the hexagonal and the orthorhombic TbPdAl undergo two successive magnetic phase transitions with the same T_N=43 K and T_t=22 K [19]. One can find that the heating and cooling *M*-*T* curves show a reversible behavior above T_N and they are not accompanied with thermal hystereses, indicating a nature of the second-order phase transition. Figures 3(a) and (b) show the temperature dependences of the magnetization at different magnetic fields. For the hexagonal HoPdAl, it is observed that the values of T_N, which depend on applied magnetic field, decrease with field increasing. However, the values of T_t remain almost unchanged. It is noticeable that the magnetization in AFM region below T_N for the hexagonal and the orthorhombic HoPdAl increase greatly with the increase of magnetic field, revealing the occurrence of a field-induced AFM-FM transition. When the applied magnetic fields are higher than about 0.2 and 1.5 T for the hexagonal and the orthorhombic HoPdAl, respectively, the magnetization as a function of temperature exhibits stepwise behavior above T_N, which corresponds to the FM-PM transition. An analogous behavior was also observed in other compounds, such as HoCuSi [13] and DySb [28].

The reciprocal magnetic susceptibility (χ^{-1}) of the hexagonal and the orthorhombic HoPdAl are plotted as a function of temperature at 0.01 T magnetic field in the insets of Figures 2(a) and (b), respectively. It is found that for the hexagonal HoPdAl, the magnetic susceptibility at temperatures above ~40 K perfectly follows the Curie-Weiss law. The PM Curie temperature (θ_p) is estimated to be 15.1 K. The value of the effective magnetic moment (μ_{eff}) per Ho ion for the hexagonal HoPdAl is obtained from the linear temperature dependence of χ^{-1} at 40–300 K to be 10.63 μ_B, which is close to μ_{eff} = 10.61 μ_B for the free Ho^{3+} ion. For the orthorhombic HoPdAl, the values of PM θ_p and μ_{eff} are 4.3 K and 10.4 μ_B, respectively, and the μ_{eff} value is slightly

smaller than that of the free Ho^{3+} ion.

Figure 4(a) shows the isothermal magnetization as a function of magnetic field for the hexagonal HoPdAl around T_N with different temperature steps in the range of 2–70 K. One can find that the isothermal *M-H* curves exhibit typical FM nature at temperatures lower than T_N and a linear relation in the PM state for temperatures much higher than T_N. However, the isothermal magnetization curves obtained well above T_C show strong curvatures at low fields as shown in other intermetallic compounds [11, 14, 29]. The curvatures in the *M-H* curves probably indicate the existence of short-range FM correlations in the PM state, which is in accordance with the result of positive θ_p (see the inset of Figure 2(a)). The positive value of θ_p implies the presence of FM interaction in the hexagonal HoPdAl compound because θ_p reflects the collective exchange interactions in the compound. The isothermal *M-H* curves were also measured respectively in the field increasing and decreasing modes around T_N in order to observe the reversibility of the magnetic transitions. There is no magnetic hysteresis in each curve, indicating that the magnetization of the hexagonal HoPdAl around T_N is perfectly reversible. Figure 4(b) shows the Arrott plots of the hexagonal HoPdAl compound at temperatures ranging from 2 to 35 K. According to the Banerjee criterion [30], a magnetic transition is expected to be of the first-order when the slope of Arrott plot is negative, whereas it will be of the second-order when the slope is positive. The positive slope above T_N indicates a characteristic of field-induced second-order PM-to-FM transition. However, it can be clearly seen from Figure 4(b) that the Arrott plots for the hexagonal HoPdAl exhibit obviously a negative slope below T_N, which confirms the occurrence of the first-order AFM-to-FM metamagnetic transition. From the isothermal *M-H* curves of the hexagonal HoPdAl below T_N (see Figure 4(a)), the critical field (B_c) required for metamagnetic transition is estimated. The value of B_c, defined as the maximum of d*M*/d*H*-*H* curve, is found to be about 0.15 T. The low B_c indicates that the hexagonal HoPdAl exhibits a weak AFM coupling, that is, the metamagnetic transition from AFM-to-FM state can be achieved by applying a very low field. Thus, the magnetization of the hexagonal HoPdAl is easily saturated below T_N. In fact, a high saturation magnetization is observed and the saturation moment in a magnetic field of 7 T at 2 K is found to be 8.9 μ_B/f.u.

Figure 5(a) shows the magnetic field dependence of magnetization for the orthorhombic HoPdAl around T_N in the temperature range of 2–40 K. It is found that the magnetizations of the orthorhombic HoPdAl below T_N increase slowly with the increase of magnetic field in a low field range owing to the existence of AFM ground state. However, it is found that the magnetization exhibits a sharp

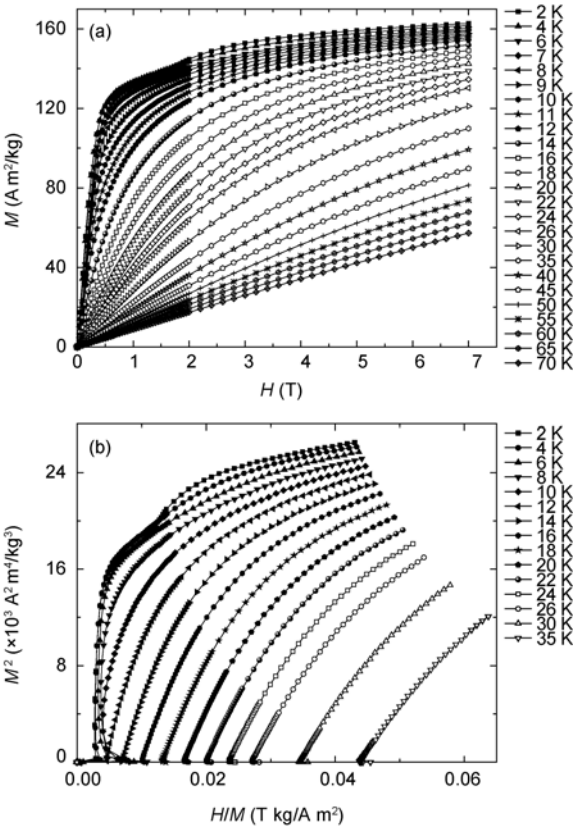

Figure 4 (a) Isothermal magnetization curves of the hexagonal HoPdAl around T_N under the magnetic fields up to 7 T and (b) Arrott plots of the hexagonal HoPdAl.

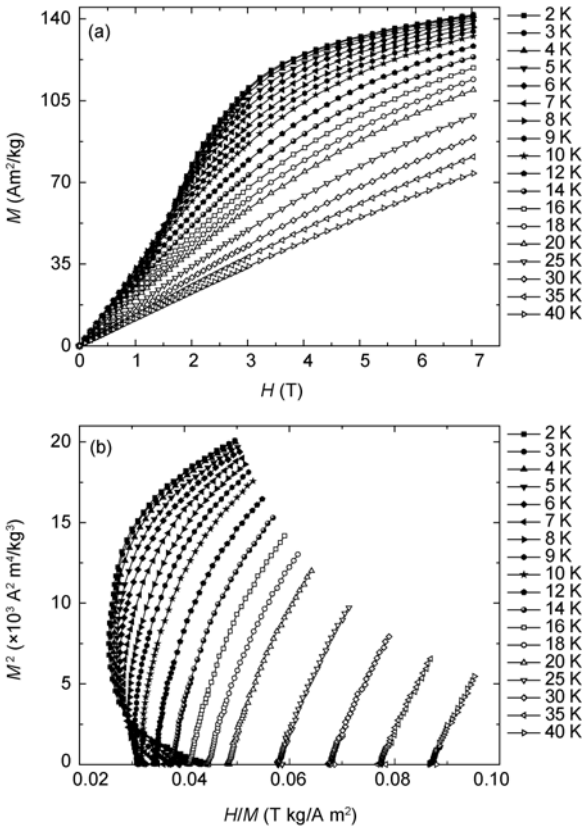

Figure 5 (a) Isothermal magnetization curves of the orthorhombic HoPdAl around T_N under the magnetic fields up to 7 T and (b) Arrott plots of the orthorhombic HoPdAl.

increase at B_c, indicating that the field-induced metamagnetic transition from AFM to FM state occurs. The Arrott plot of the orthorhombic HoPdAl (see Figure 5(b)) exhibits obviously a negative slope below T_N, confirming the existence of the field-induced first-order AFM-FM transition. Based on the isothermal *M-H* curves below T_N (Figure 5(a)), the B_C value is estimated to be 1.5 T at 2 K and has a small decrease with temperature increasing. The B_C values are much larger than those of the hexagonal HoPdAl, indicating a stronger AFM coupling in the orthorhombic HoPdAl than in the hexagonal HoPdAl. The large B_C makes the magnetization not so easy saturate even in an applied magnetic field of 7 T as shown in Figure 5(a).

In an isothermal process of magnetization, the ΔS_M of the material can be derived from Maxwell relation $\Delta S_M = \int_0^H (\partial M/\partial T)_H \mathrm{d}H$. To derive the temperature dependence of ΔS_M, the following numerical approximation of the integral is usually adopted under increasing and decreasing fields:

$$|\Delta S_M| = \sum_i \frac{M_i - M_{i+1}}{T_{i+1} - T_i} \Delta H_i, \quad (1)$$

where M_i and M_{i+1} are the experimental values of the magnetization measured at T_i and T_{i+1} in an applied magnetic field H_i, respectively. The ΔS_M for HoPdAl was calculated based on the isothermal magnetization data according to expression (1). Figure 6 shows the temperature dependence of ΔS_M around T_N for different magnetic field changes. For the hexagonal HoPdAl, it is observed from Figures 6(a) and (b) that both the heights and the width of ΔS_M peaks depend on the magnetic field applied externally, and they increase obviously with filed increasing. The ΔS_M peak is found to broaden asymmetrically toward high temperatures with the increase of magnetic field as shown in the metamagnetic La(Fe, Si)$_{13}$ compounds [6], resulting in a large MCE at temperatures above T_N. It can also be seen from Figures 6(a) and (b) that each of ΔS_M-T curve exhibits a slight bulge around T_t, which is associated with the frustrated AFM structure [24–26]. A large ΔS_M, which results from the field-induced AFM-FM metamagnetic transition, is observed in the hexagonal HoPdAl around T_N. The maximal values of $-\Delta S_M$ reach 12.8, 20.6 and 23.6 J/kg K for the sample annealed at 1080°C for 12 days (see Figure 6(a)) and 11.4, 22.8 and 27.4 J/kg K for the as-cast sample (see Figure 6(b)) under magnetic field changes of 0–2 T, 0–5 T and 0–7 T, respectively. It is found that the ΔS_M value of the hexagonal HoPdAl is comparable to those of HoCoAl [10], HoNiAl [11], Er_3Co [14], and $DyNi_2$ [15] compounds with a similar magnetic transition temperature and it is also much larger than those of DySb [28], $DyNi_5$ and $ErNi_5$ [31].

It is also found from Figure 6(c) that the values of ΔS_M of the orthorhombic HoPdAl are positive at temperatures below T_N and under lower magnetic fields, but they change into negative values with applied field increasing owing to the field-induced AFM-FM transition. The negative values of ΔS_M in the FM and the PM states result from magnetically more ordered configuration, with a magnetic field applied externally [32]. However, the positive value of ΔS_M in the AFM ordering is attributed to the disordered magnetic sublattices antiparallel to the applied magnetic field [33]. A positive value of ΔS_M for the orthorhombic HoPdAl indi-

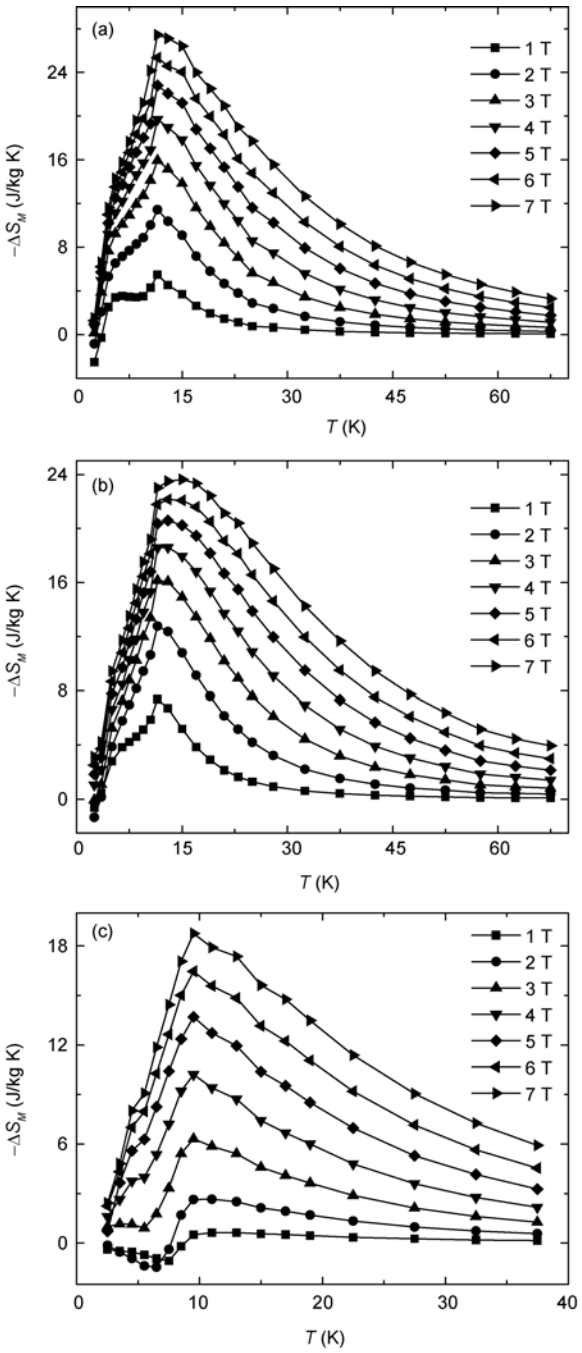

Figure 6 Temperature dependences of magnetic entropy change ΔS_M for (a) the as-cast sample of the hexagonal HoPdAl, (b) the hexagonal HoPdAl prepared by annealing as-cast sample at 1080°C for 12 days and (c) the orthorhombic HoPdAl annealed at 750°C for 50 days for different magnetic field changes.

cates a dominance of AFM ordering at low temperatures. When the temperature is increased to T_N, the field-induced AFM-FM transition leads to a large negative value of ΔS_M. The maximum value of ΔS_M is found to increase monotonically with the increase of applied magnetic field and reaches a value of −13.7 J/kg K around T_N for a magnetic field change from 0 to 5 T. The ΔS_M value is smaller than that of the hexagonal HoPdAl owing to a stronger AFM coupling in the orthorhombic HoPdAl.

The value of RC for the hexagonal HoPdAl is estimated by using the approach suggested by Gschneidner et al. [34]. The RC is defined as RC= $\int_{T_1}^{T_2} |\Delta S_M| \mathrm{d}T$, where T_1 and T_2 are the temperatures corresponding to both sides of the half-maximum value of ΔS_M peak, respectively. Calculations show that the maximal value of RC for the hexagonal HoPdAl is 386 J/kg with T_1=6.8 K (temperature of the cold reservoir) and T_2=31 K (temperature of the hot reservoir) for a magnetic field change of 0–5 T. It is evident that the large RC of HoPdAl is due to the large ΔS_M and the relatively wide ΔS_M peak.

4 Conclusion

The hexagonal and the orthorhombic HoPdAl compounds are found to exhibit a second-order AFM-PM transition at T_N =12 and 10 K, respectively, and to undergo a field-induced metamagnetic transition from AFM state to FM state below T_N. The critical field required for metamagnetic transition is estimated to be about 0.15 T, indicating that the hexagonal HoPdAl has a weak AFM coupling. Large reversible MCE is observed around T_N. The maximal value of ΔS_M is determined to be −20.6 J/kg K with a considerable RC value of 386 J/kg for a field change of 0–5 T. It is interesting that for a field change of 0–2 T, which can be supplied by a permanent magnet, the ΔS_M value for HoPdAl is as high as −12.8 J/kg K. The good magnetocaloric properties in the hexagonal HoPdAl compound result from the high saturation magnetization caused by the field-induced AFM-FM transition below T_N.

The present work was supported by the National Natural Science Foundation of China (Grant Nos. 50731007 and 51021061), the Knowledge Innovation Project of the Chinese Academy of Sciences, and the High-Technology Research and Development Program of China.

1 Tishin A M, Spichkin Y I. The Magnetocaloric Effect and its Applications. Coey J M D, Tilley D R, Vij D R, eds. Bristol: Institute of Physics Publishing, 2003
2 Gschneidner Jr K A, Pecharsky V K, Tsokol A O. Recent developments in magnetocaloric materials. Rep Prog Phys, 2005, 68: 1479–1539
3 Brück E. Handbook of Magnetic Materials. Buschow K H J, ed. Amsterdam: Elsevier B.V., 2008, Vol. 17. 235
4 Shen B G, Sun J R, Hu F X, et al. Recent progress in exploring magnetocaloric materials. Adv Mater, 2009, 21: 4545–4564
5 Pecharsky V K, Gschneidner Jr K A. Giant Magnetocaloric Effect in $Gd_5(Si_2Ge_2)$. Phys Rev Lett, 1997, 78: 4494–4497
6 Hu F X, Shen B G, Sun J R, et al. Influence of negative lattice expansion and metamagnetic transition on magnetic entropy change in the compound $LaFe_{11.4}Si_{1.6}$. Appl Phys Lett, 2001, 78: 3675–3677
7 Wada H, Tanabe Y. Giant magnetocaloric effect of $MnAs_{1-x}Sb_x$. Appl Phys Lett, 2001, 79: 3302–3304
8 Tegus O, Brück E, Buschow K H J, et al. Transition-metal-based magnetic refrigerants for room-temperature applications. Nature (London), 2002, 415: 150–152
9 Krenke T, Duman E, Acet M, et al. Inverse magnetocaloric effect in ferromagnetic NiMnSn alloys. Nat Mater, 2005, 4: 450–454
10 Zhang X X, Wang F W, Wen G H. Magnetic entropy change in RCoAl (R = Gd, Tb, Dy, and Ho) compounds: Candidate materials for providing magnetic refrigeration in the temperature range 10 K to 100 K. J Phys-Condens Matter, 2001, 13: L747–L752
11 Singh N K, Suresh K G, Nirmala R, et al. Effect of magnetic polarons on the magnetic, magnetocaloric, and magnetoresistance properties of the intermetallic compound HoNiAl. J Appl Phys, 2007, 101: 093904
12 Dong Q Y, Shen B G, Chen J, et al. Large reversible magnetocaloric effect in DyCuAl compound. J Appl Phys, 2009, 105: 113902
13 Chen J, Shen B G, Dong Q Y, et al. Giant reversible magnetocaloric effect in metamagnetic HoCuSi compound. Appl Phys Lett, 2010, 96: 152501
14 Shen J, Zhao J L, Hu F X, et al. Order of magnetic transition and large magnetocaloric effect in Er_3Co. Chin Phys B, 2010, 19: 047502
15 von Ranke P J, Pecharsky V K, Gschneidner Jr K A. Influence of the crystalline electrical field on the magnetocaloric effect of $DyAl_2$, $ErAl_2$, and $DyNi_2$. Phys Rev B, 1998, 58: 12110–12116
16 Chen J, Shen B G, Dong Q Y, et al. Large reversible magnetocaloric effect caused by two successive magnetic transitions in ErGa compound. Appl Phys Lett, 2009, 95: 132504
17 Hulliger F. On the rare-earth palladium aluminides LnPdA1. J Alloys Compd, 1995, 218: 44–46
18 Talik E, Skutecka M, Kusz J, et al. Magnetic properties of GdPdAl single crystals. J Alloys Compd, 2001, 325: 42–49
19 Dönni A, Kitazawa H, Fischer P, et al. Evidence for an isostructural phase transition in the metastable high-temperature modification of TbPdAl. J Alloys Compd, 1999, 289: 11–17
20 Talik E, Skutecka M, Kusz J, et al. Magnetic properties of DyPdAl. J Magn Magn Mater, 2004, 272-276: 767–768
21 Talik E, Skutecka M, Kusz J, et al. Electronic structure and magnetic properties of a HoPdAl single crystal. J Alloys Compd, 2003, 359: 103–108
22 Kusz J, Böhm H, Talik E, et al. Isostructural phase transition in the GdPdAl single crystals. J Alloys Compd, 2003, 348: 65–71
23 Prchal J, Javorský P, Rusz J, et al. Structural discontinuity in the hexagonal *RT*Al compounds: Experiments and density-functional theory calculations. Phys Rev B, 2008, 77: 134106
24 Javorský P, Prokleška J, Isnard O, et al. Crystal and magnetic structures in the Tb(Pd, Ni)Al series. J Phys-Condens Mater, 2008, 20: 104223
25 Dönni A, Kitazawa H, Keller L, et al. Determination of frustrated and non-frustrated magnetic structures of hexagonal and orthorhombic TbPdAl. J Alloys Compd, 2009, 477: 16–22
26 Shen J, Zheng X Q, Zhang H, et al. Metamagnetic transition and magnetocaloric effect in antiferromagnetic TbPdAl compound. J Magn Magn Mater, 2011, 323: 2949–2952
27 Klimczak M, Talik E. Magnetocaloric effect of GdTX (T = Mn, Fe, Ni, Pd, X=Al, In) and $GdFe_6Al_6$ ternary compounds. J Phys-Conf Ser, 2010, 200: 092009
28 Hu W J, Du J, Li B, et al. Giant magnetocaloric effect in the Ising antiferromagnet DySb. Appl Phys Lett, 2008, 92: 192505
29 Arora P, Tiwari P, Sathe V G, et al. Magnetocaloric effect in $DyCu_2$. J Magn Magn Mater, 2009, 321: 3278–3284
30 Banerjee S K. On a generalised approach to first and second order magnetic transitions. Phys Lett, 1964, 12: 16
31 von Ranke P J, Mota M A, Grangeia D F, et al. Magnetocaloric effect in the RNi_5 (R=Pr, Nd, Gd, Tb, Dy, Ho, Er) series. Phys Rev B, 1998, 70: 134428
32 Samanta T, Das I. Negligible influence of domain walls on the magnetocaloric effect in $GdPt_2$. Phys Rev B, 2006, 74: 132405
33 Samanta T, Das I, Banerjee S. Giant magnetocaloric effect in antiferromagnetic $ErRu_2Si_2$ compound. Appl Phys Lett, 2007, 91: 152506
34 Gschneidner Jr K A, Pecharsky V K, Pecharsky A O, et al. Recent developments in magnetic refrigeration. Mater Sci Forum, 1999, 315: 69